Global Scientific JOURNALS

GSJ: Volume 6, Issue 5, May 2018, Online: ISSN 2320-9186

www.globalscientificjournal.com

BER ESTIMATION IN A CHROMATIC DISPERSION CO-OFDM DUAL POLARIZATION BASED SYSTEMS

Ishiwu I. Jude
Department of Electrical/Electronics Engineering
Modibbo Adama University of Technology, Yola Adamawa State, Nigeria
judeclinton30@gmail.com

Yahya Adamu
Department of Electrical/Electronics Engineering
Modibbo Adama University of Technology, Yola Adamawa State, Nigeria
adamuyahya2002@yahoo.com

Oguche D. Onoja
Department of Electrical/Electronics Engineering
Modibbo Adama University of Technology, Yola Adamawa State, Nigeria
onojaforyou@yahoo.com

Jonathan Yakubu
Department of Electrical/Electronics Engineering
Modibbo Adama University of Technology, Yola Adamawa State, Nigeria
jona4me@yahoo.com

***Abstract*:** We present experimental demonstrations using both Coherent and Direct-Detection Optical-Orthogonal Frequency Division Multiplexing (DDO-OFDM and CO-OFDM) for the compensation of Chromatic Dispersion (CD) and residual dispersion in long-haul optical fiber networks. The analysis showed that CO-OFDM outperformed that of DDO-OFDM provided the same parameters were used throughout the experiments. Two model systems were developed, one with Phase Rotation Method/Constellation Adjustment Method (PRM/CAM) and one without. From the results obtained, it showed that the model with PRM outperformed one without PRM. Different modulation formats (Quadrature Phase Keyings and Quadrature Amplitude Modulations) were used in the simulations, the results obtained equally showed that the lower modulation schemes; QPSK and 4-QAM have a better BERs than the higher modulation schemes; 256-QAM and 512-QAM. At a high distance of about 1000 km, the 4-QAM systems outperformed QPSK, 256-QAM and 512-QAM system by a factor of 10^{-2}, 10^{-4} and 10^{-5} respectively.

Keywords: BER, Chromatic Dispersion, DDO-OFDM, CO-OFDM, Cyclic Prefix, DSP.

1. INTRODUCTION

Orthogonal Frequency Division Multiplexing (OFDM) is a robust digital modulation technique widely used in most recent and advanced broadband communication systems[1]. It is the basic technology behind the LTE, LTE-Advance/Fourth Generation (4G) and the future Fifth Generation (5G) networks [2]. In an OFDM system, a closely-spaced, huge number of subcarriers are used to transmit data, this is achieved by dividing the whole data streams into multiple parallel small sub-streams/channels and allocating a sub channel for each of the sub streams [3]. Finally, each of these subcarriers are modulated with appropriate modulation techniques such as; M-arrays Quadrature Amplitude Modulation (M-QAM) and M-arrays Phase Shifting Keying (M-PSK) at a very low symbol rate other than the conventional single carrier modulation scheme like Frequency Division Multiple Access (FDMA), achieving it under the same bandwidth [3].

In a broad view, OFDM is a multicarrier transmission technique, which divides an allocated spectrum into many carriers, each one being modulated by a low rate data stream [1]. In comparison, OFDM is similar to FDMA in that the multiple user access is achieved by subdividing the available bandwidth into multiple channels, which are then allocated to different users. Economically, OFDM offers more benefits in utilization of available bandwidth than FDMA. This is because it uses the spectrum much more efficiently by spacing the channels much closer together [4]. Although, it achieved this by making all the carriers orthogonal to one another, thereby preventing interference between the closely spaced carriers. OFDM subcarriers overlap each other, though they interfere with each other due to the orthogonality (perpendicular) nature of each subcarriers [5].

2. FIBER WORKING PRINCIPLE

When the input data, in the form of electrical signals, is given to the transmitter circuitry, it converts them into light signal with the help of a light source. This source is of Light Emitting Diode (LED) whose amplitude, frequency and phases must remain stable and free from fluctuation in order to have efficient transmission [6]. The light beam from the source is carried by a fiber optic cable to the destination circuitry wherein the information is transmitted back to the electrical signal by a receiver circuit [7].

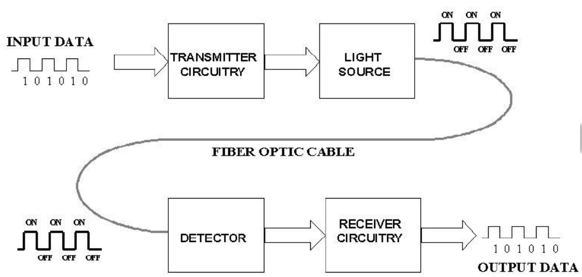

Fig. 1 Working Principle of Fiber Communication

The Receiver circuit consists of a photo detector along with an appropriate electronic circuit, which is capable of measuring magnitude, frequency and phase of the optic field. This type of communication uses the wave lengths near to the infrared band that are just above the visible range [8]. Both LED and Laser can be used as light sources based on the application. At the receiver, the exact information transmitted are distorted by phase noise, interference and other fiber impairments. In this paper, we were able to minimize or rather proffer a solution in tackling of these impairments.

2.1 Cyclic Prefix (CP) for OFDM

One of the enabling techniques for the mitigation of dispersive channel effects such as Chromatic Dispersions (CP) and polarization dispersions mode is the insertion of the cyclic prefix [9]. Though, other additional techniques in OFDM such as modulation and demodulation of many orthogonal subcarriers via; FFT and IFFT are done for a better signal performance [10]. Here, we consider two consecutive OFDM symbols that undergo a dispersive channel with a delay spread of t_d. For clarity, each OFDM symbol includes only two subcarriers with a fast delay and slow delay spread at t_d, represented by "fast subcarrier" and "slow subcarrier," respectively. Figure 2(a) shows that inside each OFDM symbol, the two subcarriers, "fast subcarrier" and "slow subcarrier" are aligned upon the transmission. Figure 2(b) shows the same OFDM signals upon the reception, where the "slow subcarrier" is delayed by t_d against the "fast subcarrier." A DFT window is been selected containing a complete OFDM symbol for the "fast subcarrier." It is perceived that due to the channel dispersion, the "slow subcarrier" has crossed the symbol boundary leading to the interference between neighbouring OFDM symbols, formally, the so-called Inter Symbol Interference (ISI) [11]. Moreover, the OFDM waveform in the DFT window for "slow subcarrier" is incomplete, the critical orthogonality condition for the subcarriers is lost, resulting in an Inter Carrier Interference (ICI) penalty.

Cyclic prefix was a good technique proposed to resolve the channel dispersion-induced ISI and ICI [12, 13]. Figure 2(c) shows insertion of a cyclic prefix by cyclic extension of the OFDM waveform into the guard interval G. As we can see from Fig. 2(c), the waveform in the guard interval is essentially an identical copy of that in the DFT window, with time-shifted by "t_s" forward. Figure 2(d) shows the OFDM signal with the guard interval upon reception. We make two assumptions here; that the same signal has traversed the same dispersive channel, and the same DFT window is selected containing a complete OFDM symbol for the "fast subcarrier" waveform. It can be seen from Figure 2(d), that a complete OFDM symbol for "slow subcarrier" is also maintained in the DFT window, because a proportion of the cyclic prefix has moved into the DFT window to replace the identical part that has shifted out. As such, the OFDM symbol for "slow subcarrier" is an "almost" identical copy of the transmitted waveform with an additional phase shift. This phase shift is dealt with through channel estimation and will be subsequently removed for symbol decision [14].

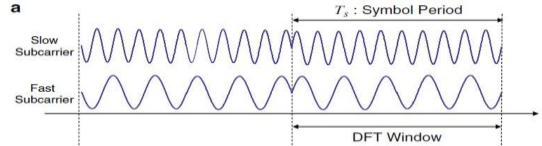

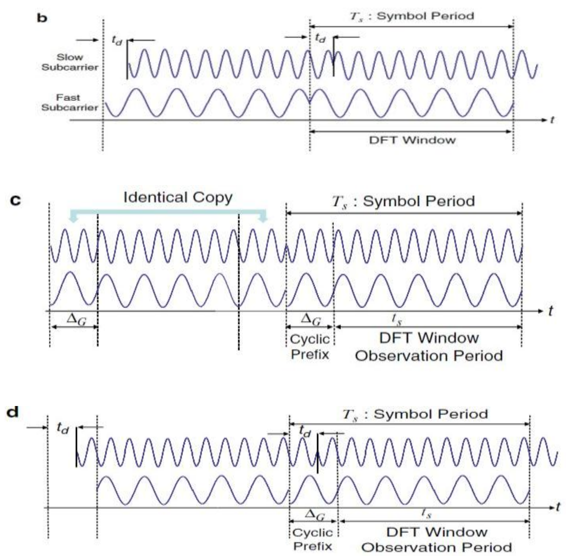

Fig. 2.10 OFDM signals (a) without Cyclic Prefix at the transmitter, (b) without Cyclic Prefix at the receiver, (c) with Cyclic Prefix at the transmitter (d) with Cyclic Prefix at the receiver

The important condition for ISI-free OFDM transmission is given by:

$$td < \Delta G: \qquad 1$$

It can be seen that after insertion of the guard interval greater than the delay spread, two critical procedures must be carried out to recover the OFDM information symbol properly, namely, (a) selection of an appropriate DFT window, called DFT window synchronization, and (b) estimation of the phase shift for each subcarrier, called channel estimation or subcarrier recovery. Both Digital Signal Processing (DSP) procedures are actively pursued research topics, and their references can be found in both books and journal papers [15].

Figure 3 illustrates one complete OFDM symbol composed of observation period and cyclic prefix corresponding time-domain OFDM symbol. The waveform within the observation period will be used to recover the frequency-domain information symbols [16].

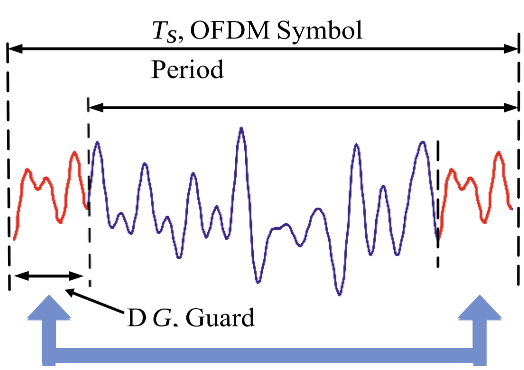

Fig. 3 Time-domain OFDM Signal for a Complete OFDM Symbol.

2.2 Optical Single Side Band (OSSB) Signal Generation Implementing a Bragg Grating

In the mid-1990s, different authors have proposed on the use of chirped Fiber-Bragg Grating (FBG) to compensate for Chromatic Dispersion (CD) penalty. Recently, an experiment on a Reduction of Chromatic Dispersion Effect in Lightwave Microwave/Millimeter-Wave Transmission using Tapered Linearly Chirped Fiber Grating [17]. It was found that the generation of Optical Single Sideband + Carrier (OSSB + Carrier) instead of conventional Optical Double Sideband (ODSB) signal eliminates the power fading phenomenon, since the detected RF power results from only one beat signal. Optical filtering was used to eliminate one of the two sidebands of the optical spectrum. The key reason for the filtering when applied for baseband transmission was for the compensation of CD in a long-haul transmission [18].

Then, [19] extended OSSB filtering to fiber-radio system and equally used Fiber Bragg-Grating to filter out one sideband of ODSB signal. The experiment was conducted using a transmission of 25GHz RF signal over a 51km Long SSMF link, leading a progressive result of no fading of the photo-detected power level. The shortfall emanated from this work is that the filtering technique is quite dependent on the wavelength of the optical carrier leading to an imperfect compensation of CD. Although, implementation is very easy, it requires a narrow bandwidth optical filter. Similarly, the effect of residual dispersion that remains after chromatic dispersion and equalization have been analyzed in a journal paper title, Efficient Chromatic and Residual Dispersion Postcompensation for Coherent Optical OFDM. It was observed that OFDM systems with CAM shows a superior Min BERs than the Non-Return-to-Zero (NRZ) systems [20].

3. EXPERIMENTAL PROCEDURE

Firstly, an O-OFDM model is developed using an OptiSystem Software. OptiSystem is an innovative, rapidly evolving, and powerful software design tool that enables users to plan, test, and simulate almost every type of optical link in the transmission layer of a broad spectrum of optical networks from LAN, MAN to ultra-long-haul transmission. The next step is to incorporate O-OFDM detection techniques; CO-OFDM and DD-OFDM into the O-OFDM model. The first simulation is carried out using both techniques and we compare their percentage (%) Min-BER improvement with and without CAM. The second simulation is carried out using different CO-OFDM modulation techniques and we compare their Min-BERs with and without Phase Rotation Method (PRM) at different stages as the distance increases. Finally, analysis of the performance results were carried out using MATLAB technical computing package.

3.1 System Setup

Both DDO-OFDM and CO-OFDM system includes five basic functional blocks as shown in Figure 3 below: OFDM transmitter, RF to Optical up-converter, optical link, Optical to RF (OTR) down-converter, and OFDM receiver [21].

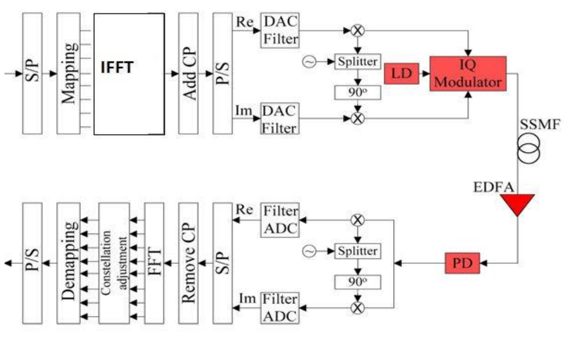

Fig. 3 A Schematic of DDO-OFDM System Setup

The only different in both circuits are replacing the Mach Zhender Modulator (MZM) and PIN detector in DDO-OFDM with optical In-Phase/Quadrature (I-Q) modulator and coherent receiver respectively [22]. However, both techniques have their own peculiar advantages and disadvantages. In DD-OOFDM the receiver is simple, but some optical frequencies must be unused if unwanted mixing products are not to cause interference. Although, this is usually achieved by inserting a guard band between the optical carrier and the OFDM subcarriers, which resulted in reducing the spectral efficiency. The shortfall of DD-OOFDM is that more transmitted optical power is required for carrier transmission. Nevertheless, CO-OFDM requires a laser at the receiver to generate the carrier locally, even though, it`s more sensitive to phase noise.

3.2 Phase Rotation Method (PRM)

Phase Rotation Method (PRM), which in other way round is the same as Constellation adjustment method (CAM) is a method used in tackling some Residual Dispersion left after chromatic dispersion and equalization. The essence of measured constellation diagrams representation is to recognize the type of interference and distortion in a signal. Here, we represent our signal as a two-dimensional xy-planes scatter diagram in a complex plane at a symbol sampling instant as shown is in Figure 4 below;

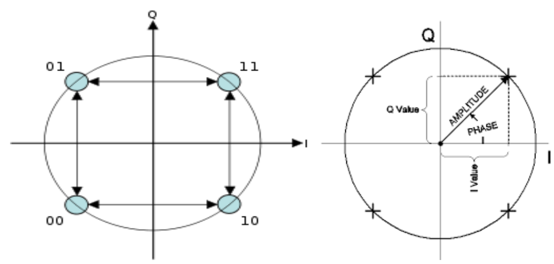

Fig. 4 Two-dimensional xy-planes scatter diagram

However, upon reception of the signal, the demodulator will examine the received symbol, which invariable may have been corrupted by distortion, chromatic dispersion, Additive White Gaussian Noise (AWGN), phase noise, inter-symbol and inter-carrier interferences. The demodulator selects, as well as estimate exactly what was actually transmitted, at that point on the constellation diagram which is closest to that of the received symbol. For that reasons, it will demoulate incorrectly due the corruption encountered. The received symbol will move closer to another constellation points than the actual estimated points. Figure 5 below show the direction phase rotation from the received points to exact points in the xy-planes.

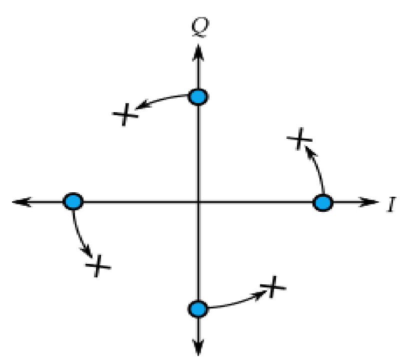

Fig. 5 Direction of Phase Rotation in IQ-plane

However, with the signal encountering some impairments, we use Phase Rotation Method as outlined below to tackle it; We first rotate the phase dispersion $\Theta_{(k)}$ for all the subcarriers, divide the constellation points into four quadrants for 4-QAM, eight quadrants for 8-QAM, sixteen quadrants for 16-QAM and so on, each according to the subcarrier modulation format. The next step is for each the four quadrant, we calculate the centre of the points, with each of the four carrier signals as below;

$$S_{0(t)} = A_c \, Cos\,(2\pi f_0 t + 0) \rightarrow 00 \quad (2)$$

$$S_{1(t)} = A_c \, Cos\,(2\pi f_0 t + \frac{\pi}{2}) \rightarrow 01 \quad (3)$$

$$S_{2(t)} = A_c \, Cos\,(2\pi f_0 t + \pi) \rightarrow 10 \quad (4)$$

$$S_{3(t)} = A_c \, Cos\,(2\pi f_0 t + \frac{3\pi}{2}) \rightarrow 11 \quad (5)$$

The difference between the estimated phase/amplitude and the theoretical constellation positions are tabulated. We make an adjustment to all subcarriers in each quadrants to compensate the phase/amplitude discrepancies. The procedure is repeated until there exist no discrepancies among the amplitude/phase angles. Below is the flow chart for the Phase Rotation Method described above.

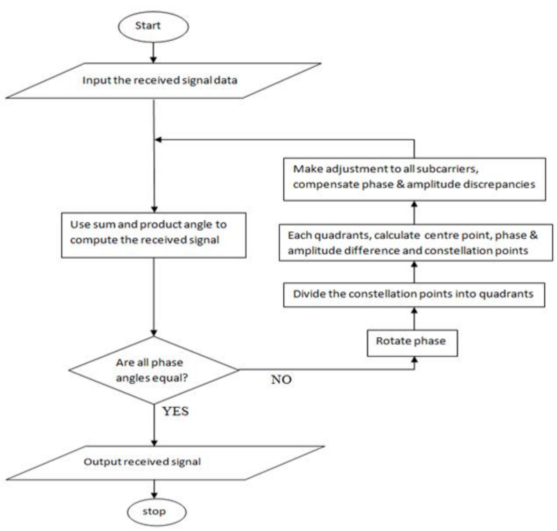

Fig. 6 Flow Chart for Phase Rotation Method

3.3 Parameters Used for Simulations

The general parameters used for this simulation are shown in Table 1 below, while Table 2 and 3 show the Transmitter/Receiver Parameters, Optical Fiber Link Parameters and Receiver Parameters respectively;

Table 1 Simulation Parameters

S/No	Parameters	Values	Units
1	Bit rate	10e9	bit/sec
2	Time window	12.8e-9	Sec
3	Sample rate	640e9	Hz
4	Sequence length	128	Bits
5	Samples per bit	64	
6	Symbol rate	10e9	Symbols/sec
7	Sensitivity	-100	dB
8	Resolution	0.1	Nm
9	Interpolation offset	0.5	Nm

Table 2 Transmitter/Receiver Parameters

S/No	Parameters	Values	Units
1	QAM Bits Per Symbol (b/sym)	2	Bits
2	QAM Gray Code	No	
3	QAM Differential Coding	No	
4	OFDM Size	144	
5	OFDM Maximum possible subcarriers	128	
6	OFDM Guard interval	16	
7	OFDM used subcarrier	82	
8	OFDM unused subcarrier	41	
9	OFDM Pilot subcarrier	5	
10	Average OFDM power	12	dBm
11	CW Laser frequency	193.1	THz
12	CW Laser power	10	dBm
13	CW Laser linewidth	0.1	MHz
14	CW Laser Azimuth	45	Degree
15	LPBF Cut-off frequency	0.75 x Symbol rate	Hz

Table 3 Optical Fiber Link Parameters

S/No	Parameter	Value	Units
1	Optical fiber length	100 - 1000	Km
2	Attenuation	0.2	dB/km
3	Dispersion	17	Ps/nm/km
4	Effective area	80	μm^2
5	Reference wavelength	193.1	THz
6	Optical gain	20	dB
7	Optical noise figure	4	dB
8	Ideal Dispersion Compensation FBG Bandwidth	125	GHz
9	Dispersion	-800	Ps/nm

3.4 Coherent Optical-OFDM Transmitter

The transmitter system model consist of two parts, namely; RF transmitter and Optical transmitter. The optical transmitter converts the electrical signal into optical form and lunch the resulting optical signal into the fiber optical link. The optical transmitter consists of three components, namely; optical source, electrical pulse generator and optical modulator. Here, both modulation and multiplexing are achieved digitally using an Inverse Discrete Fourier Transform (IDFT). Note that, the subcarrier frequencies are mathematically orthogonal over one OFDM symbol period. Figure 7 depicted the simulation set-up for the 4-QAM CO-OFDM Transmitter. While Figure 6 depicted A Coherent 16 QAM 4 Level Circular Dual Polarization (DP) Transmitter as well.

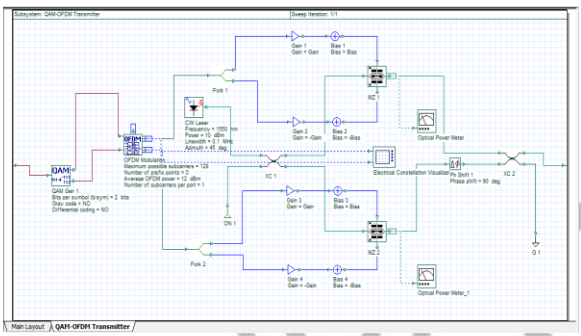

Fig. 7 4-QAM CO-OFDM Transmitter

112-Gb/s (112x1000-Mb/s) CO-OFDM super-channel signal is generated by multiplexing five (5) OFDM sub-bands. Each band consists 22.4-Gb/s OFDM signals which are transmitted in dual polarizations. The QAM CO-OFDM transmitter has a gain and bias of 0.021 volt and 1.5 volt respectively and an optical frequency source with a Continuous Wave (CW) laser of 191.1THz and 10 dBm for optical frequency and power respectively. The transmitted signal is generated off-line by a Pseudo-Random Bit Sequence (PRBS) Generator with $10e^9$ bits/secs, Time window of $3.2768e^{-6}$ s, Sample rate of $10e^{-}9$ Hz and Symbol rate of $5e^9$ Symbols/s and mapped to 16-QAM constellation. The digital time domain signal is formed after IFFT operation. The FFT size of OFDM is 128 carriers, and guard interval is 1/8 of the symbol window. The middle 82 subcarriers out of 128 are filled, from which five pilot subcarriers are used for phase estimation.

3.5 Optical Fiber Link

The Fiber Link for CO-OFDM set-up consists of 100 km span of Standard Single Mode Fiber (S-SMF) including an Ideal Dispersion Compensation Fiber Bragg Grating (FBG) and Optical Amplifier prior to each span. Figure 8 shows the configuration of the fiber link. The Optical Amplifier increases the link distance, which is limited by fiber loss in an optical communication system. The length of fiber can be increased by increasing the number of loops. The amplifiers have a 4-dB noise figure and a 20-dB gain, while the Optical Fiber has a dispersion of 17 ps/nm/km, an effective area of 80 μm^2, attenuation of 0.2-dB/km and reference wavelength of 193.1THz.. The ideal dispersion compensation Fiber Bragg Gratings (FBGs) have a frequency of 193.1 THz, bandwidth of 125 GHz, dispersion of -800 ps/nm and a noise threshold of about -100 dB.

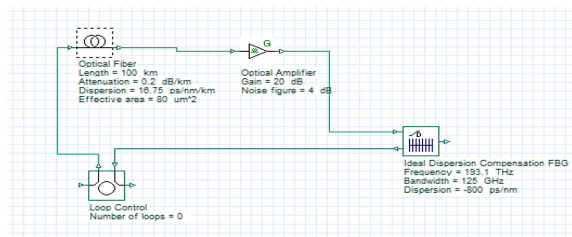

Fig. 8 Architecture of CO-OFDM Fiber Link.

3.6 Coherent Optical-OFDM Receiver

The 4-QAM CO-OFDM Receiver side comprises a polarization beam splitter, a local laser, two optical 90^0 hybrids, and four balanced photo-receivers are used to down-convert the data to the RF domain. Figure 9 shows the schematic of Coherent Optical-OFDM receiver.

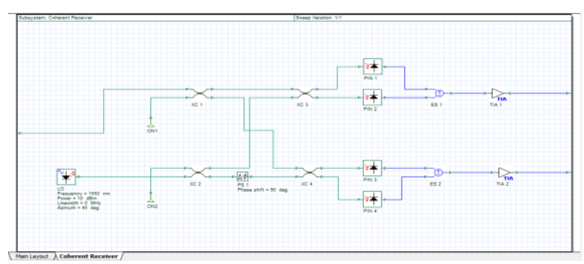

Fig. 9 A 4-QAM CO-OFDM Receiver

The complete architecture of the 112 GB/s 4-QAM DDO-OFDM Post-Compensation Fiber Bragg Grating (FBG) is shown in Figure 10 below;.

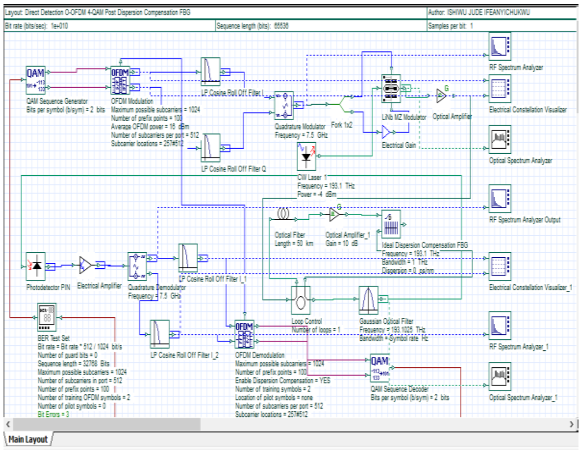

Fig. 10 Architecture of 112-GB/s 4-QAM DDO-OFDM Post-Compensation Fiber Bragg Grating.

4. SIMULATION RESULTS

Both DDO-OFDM and CO-OFDM 112-GB/s Post-Compensation Fiber Bragg Grating (FBG) System where simulated and their estimated results were tabulated as shown in Tables 4-7. As earlier mentioned, the only different between the DDO-OFDM and CO-OFDM are replacing the Mach Zhender Modulator (MZM) and PIN detector in DDO-OFDM with optical In-Phase/Quadrature (I-Q) modulator and coherent receiver respectively. While Figures 11, 12, 13, 14 and 15 shows the Oscilloscope Visualizer, RF Spectrum Analyzer, Optical Spectrum Analyzer, Electrical Constellation Visualizer before CD, Electrical Constellation Visualizer after CD respectively and BER Analyzer Eye Diagram.

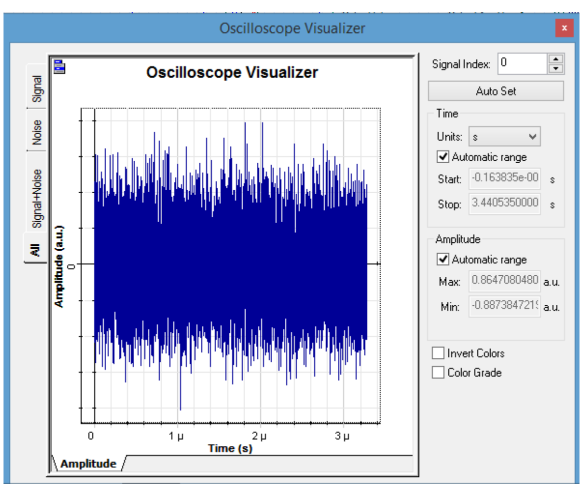

Fig. 11 Oscilloscope Visualizer

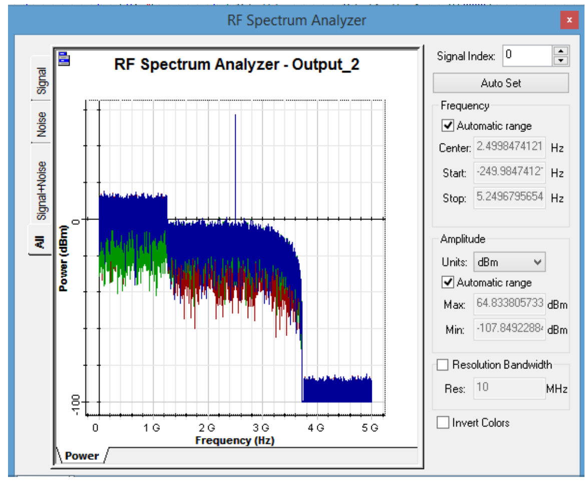

Fig. 12 RF Spectrum Analyzer

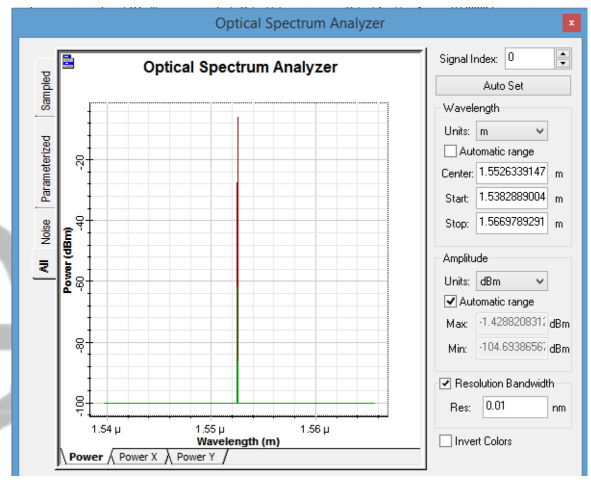

Fig. 13 Optical Spectrum Analyzer

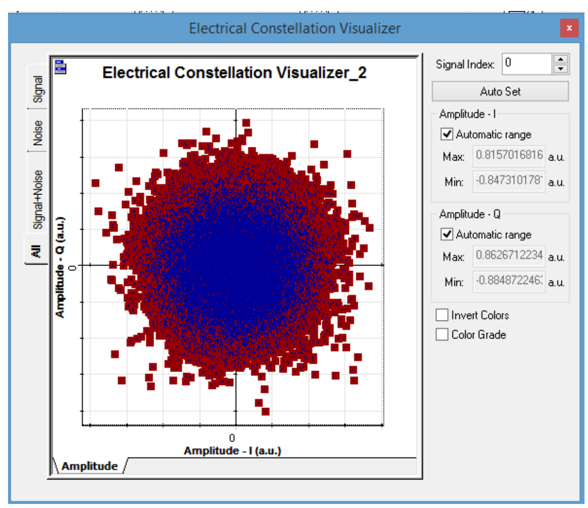

Fig. 14 Electrical Constellation Visualizer before CD

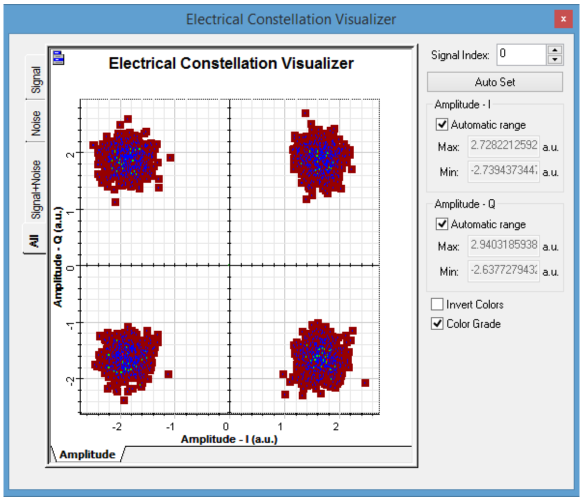

Fig. 15 Electrical Constellation Visualizer after CD

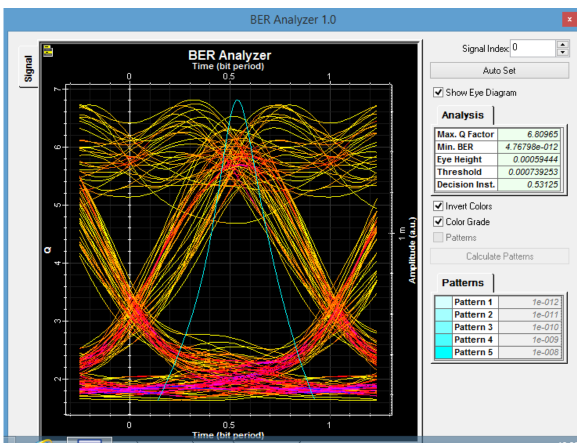

Fig. 16 BER Analyzer Eye Diagram.

4.1 Comparison of BER Improvement for DDO-OFDM and CO-OFDM

The BERs of all the various modulation systems (m-QAM and n-PSK) in DDO-OFDM against the CO-OFDM were estimated. The CO-OFDM has 2 x 7.5 GHz Low Pass Bessel Filter, four (4) PIN Detectors and IQ-Phase, while the DDO-OFDM has a PIN Detector and MZM.

The Min-BERs and their corresponding Max-Q Factors for both systems with and without Constellation Adjustment Method (CAM) were estimated as shown in Table 4 and 5 respectively. From the estimated values, we deduced the percentage (%) Min-BERs improvement (sensitivity) in each of the system over a bandwidth of 12.5 GHz for both low and high rate modulation schemes over a distance of 100 Km.

Table 4 Results Showing DD-OFDM Q-Factors and BERs Improvement.

S/No	Modulation Types	Max-Q Factors	Max-Q Factors (with CAM)	Min-BERs	Min-BERs (with CAM)	% BER Improvement
1	BPSK	3.4461	6.3993	$1.0679e^{-10}$	$5.7473e^{-9}$	85.7
2	QPSK	3.3617	6.1889	$8.1701e^{-9}$	$4.4379e^{-9}$	84.1
3	4-QAM	3.3355	6.0907	$5.6728e^{-9}$	$3.1064e^{-9}$	82.6
4	8-QAM	3.2186	5.8256	$3.1882e^{-9}$	$1.7614e^{-9}$	81.0
5	16-QAM	3.1375	5.6287	$5.7226e^{-8}$	$3.1899e^{-8}$	79.4
6	32-QAM	3.0409	5.4068	$3.1279e^{-8}$	$1.7592e^{-8}$	77.8
7	64-QAM	2.9589	5.2107	$1.0892e^{-8}$	$6.1851e^{-7}$	76.1
8	128-QAM	2.8657	5.0064	$7.9701e^{-7}$	$4.5622e^{-7}$	74.7
9	256-QAM	2.8268	4.8903	$5.4032e^{-7}$	$3.1232e^{-7}$	73.0
10	512-QAM	2.7633	4.7391	$3.0017e^{-7}$	$1.7503e^{-7}$	71.5

Table 5 Results Showing CO-OFDM Q-Factors and BERs Improvement.

S/No	Modulation Types	Max-Q Factors	Max-Q Factors (with CAM)	Min-BERs	Min-BERs (with CAM)	% BER Improvement
1	BPSK	3.5633	7.1157	$9.8240e^{-12}$	$3.8916e^{-12}$	99.7
2	QPSK	3.4941	6.9602	$7.7521e^{-12}$	$4.9194e^{-12}$	99.2
3	4-QAM	3.4289	6.8097	$4.7698e^{-12}$	$2.4010e^{-12}$	98.6
4	8-	3.39	6.66	8.44	4.30	96.1

	QAM	64	04	12e^{-11}	45e^{-11}	
5	16-QAM	3.3575	6.5020	5.1005 e^{-11}	2.5839e^{-11}	93.7
6	32-QAM	3.3549	6.3506	5.9843e^{-10}	3.1613e^{-10}	89.3
7	64-QAM	3.3267	6.1877	1.6382 e^{-10}	8.8081e^{-9}	86.0
8	128-QAM	3.2479	6.0054	6.0792e^{-9}	3.2878e^{-9}	84.9
9	256-QAM	3.2113	5.8703	2.8341 e^{-9}	1.5504e^{-9}	82.8
10	512-QAM	3.1658	5.7111	7.1059e^{-8}	3.9387e^{-8}	80.4

Comparing Table 4 and 5 above, we deduced the following;

1. The BERs improvement in CO-OFDM shows superiority than the DDO-OFDM as can be seen from both tables above. This is as a result of inherent advantages associated with CO-OFDM system, such as (a) High spectral efficiency; (b) Robust to chromatic dispersion and polarization-mode dispersion; (c) High receiver sensitivity; (d) Dispersion Compensation Modules (DCM)-free operation; (e) Less DSP complexity; (f) Less oversampling factor; (g) More flexibility in spectral shaping and matched filtering..

2. The lowest modulation rate in both table above, BPSK has a BER improvement of about 99.7% on CO-OFDM as compared to its counterpart in DDO-OFDM with BER improvement of about 85.7%. This leads to about 14.0% different in both detection techniques.

3. Similarly, the highest modulation rate in both table above show that, 512-QAM has a BER improvement of about 80.4% on CO-OFDM as against its counterpart DDO-OFDM with a BER improvement of about 71.5%, leading to 8.9% different in both.

4. The Q-factor too deteriorate as the distance of transmission increases as can be seen from both tables above.

4.2 Simulation Results of CO-OFDM at Different Loops (Distances)

The statistical analysis and results of the Min. BERs for different distances after incorporating a dispersion management scheme; dispersion compensation fiber of 16.75 Ps/nm/km with optical fiber gain and noise figure of 20dB and 4dB respectively into the coherent OFDM simulator. The simulation is done to evaluate the performances of the low rate (QPSK and 4-QAM) against the higher rate modulations (256-QAM and 512-QAM) in both CO-OFDM without CAM and CO-OFDM with CAM system. The following values were tabulated as shown in Table 6 and 7 below. Note; in each of the loops (multiple of 100km), the simulation is done for 10 iterations and the Min. BERs were recorded.

Table 6 BER Results of CO-OFDM Without CAM.

S/No	Distances (km)	Min-BERs			
		Low Rate Modulation		High Rate Modulation	
		QPSK	4-QAM	256-QAM	512-QAM
1	100	4.9194 e^{-12}	2.4010 e^{-12}	2.5504 e^{-9}	3.9387 e^{-8}
2	200	2.0079 e^{-12}	1.2099 e^{-11}	1.8674 e^{-8}	1.5081 e^{-7}
3	300	9.4215 e^{-11}	5.6501 e^{-11}	9.3950 e^{-8}	7.2568 e^{-7}
4	400	6.9437 e^{-10}	2.6730 e^{-10}	5.7801 e^{-7}	2.9014 e^{-6}
5	500	5.9802 e^{-9}	8.8214 e^{-10}	3.9063 e^{-6}	9.9523 e^{-6}
6	600	7.3247 e^{-8}	4.1175 e^{-9}	1.9040 e^{-5}	6.1569 e^{-5}
7	700	8.1077 e^{-7}	1.9832 e^{-8}	8.4303 e^{-5}	5.2017 e^{-4}
8	800	5.2708 e^{-6}	7.8178 e^{-8}	6.0677 e^{-4}	4.7708 e^{-3}
9	900	4.6710 e^{-5}	4.7067 e^{-7}	5.1173 e^{-3}	9.4367 e^{-2}
10	1000	5.1374 e^{-4}	2.9047 e^{-6}	9.0472 e^{-2}	7.9941 e^{-1}

Table 7 BER Results of CO-OFDM with CAM.

S/No	Distances (km)	Min-BERs			
		Low Rate Modulation		High Rate Modulation	
		QPSK	4-QAM	256-QAM	512-QAM
1	100	2.7521 e^{-12}	1.7698 e^{-12}	1.5341 e^{-9}	2.1059 e^{-8}
2	200	7.9147 e^{-12}	5.2478 e^{-12}	1.0013 e^{-8}	7.1171 e^{-8}
3	300	3.2204 e^{-11}	1.8100 e^{-11}	4.4050 e^{-8}	2.3567 e^{-7}
4	400	8.5010 e^{-11}	6.5175 e^{-11}	1.8701 e^{-7}	8.9342 e^{-7}
5	500	3.8371 e^{-10}	2.0210 e^{-10}	7.2131 e^{-7}	2.6320 e^{-6}
6	600	1.8353 e^{-10}	6.6512 e^{-10}	2.1047 e^{-6}	7.5072 e^{-6}
7	700	8.4477 $2e^{-9}$	2.3157 e^{-9}	6.7518 e^{-6}	2.7810 e^{-5}
8	800	4.6031 e^{-8}	6.1172 e^{-9}	1.6574 e^{-5}	9.3671 e^{-5}
9	900	3.1370 e^{-7}	2.1318 e^{-8}	5.0781 e^{-5}	2.8893 e^{-4}
10	1000	2.0029 e^{-6}	7.2461 e^{-8}	1.5193 e^{-4}	1.1192 e^{-3}

The results above were plotted using MATLAB for each of the modulation systems. Figure 17-20 show the Bit Error Rates (dB) as against the Distances (Km).

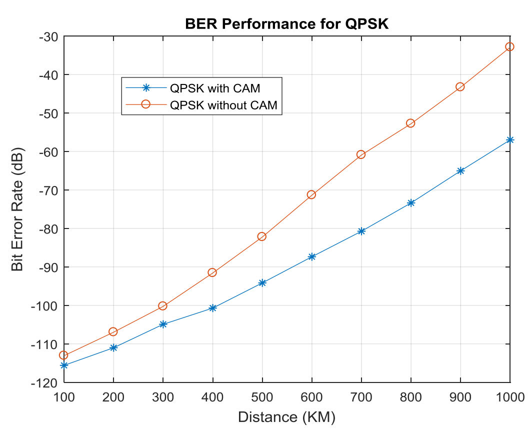

Figure 17 BERs Performance of QPSK v/s Distance for OFDM System.

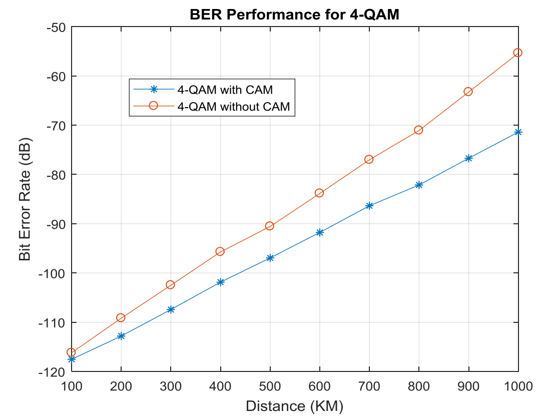

Figure 18 BERs Performance of 4-QAM v/s Distance for OFDM System.

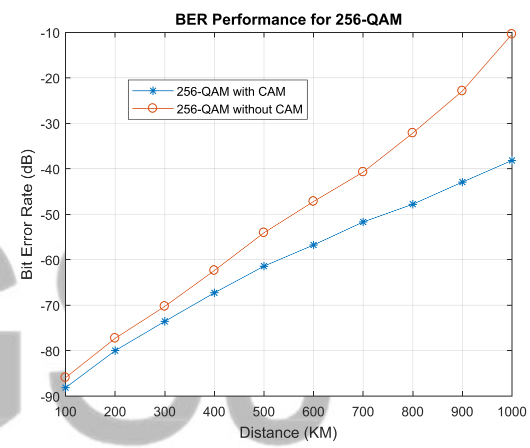

Figure 19 BERs Performance of 256-QAM v/s Distance for OFDM System.

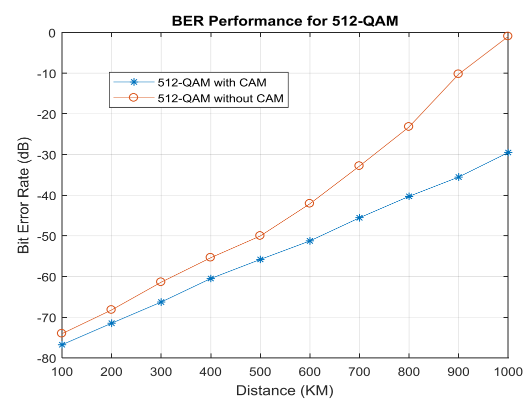

Figure 20 BERs Performance of 512-QAM v/s Distance for OFDM System.

From the simulation result shown in Table 6 and 7, we deduced the following;

1. Looking at Figure 17-20, the CO-OFDM systems with CAM/PRM outperformed the CO-OFDM without CAM/PRM.

2. In both low and high rate modulation, a better signal quality is gotten at a closer distance but degrades as the distance increases. This is as a result the susceptibility of the high rate modulation signals to chromatic and residual dispersion than the low rate. Although, low rate modulations have poor bandwidth efficiency and low speed than the high rate.

However, the next step is to compare the performance analysis of the four modulation systems; QPSK, 4-QAM, 256-QAM and 512-QAM CO-OFDM with CAM, we deduced the following from Figure 21 below.

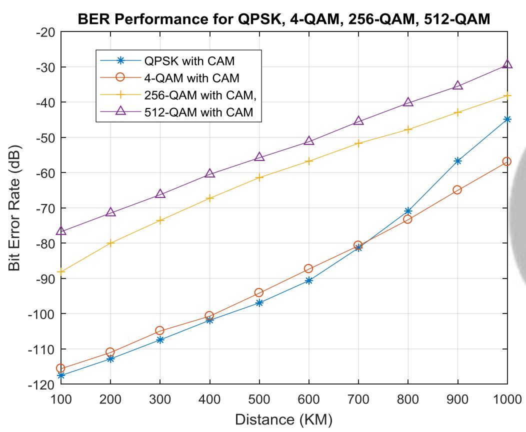

Figure 21 BERs Performance of QPSK, 4-QAM, 256-QAM and 512-QAM v/s Distance.

1. At a distance of 1000 km, the 4-QAM systems outperformed QPSK, 256-QAM and 512-QAM system by a factor of 10^{-2}, 10^{-4} and 10^{-5} respectively. This is a result of the inability of the trios to overcome the residual dispersion left after chromatic dispersion at a higher distance.

2. Secondly, at a distance of about 700 Km, the BERs improvement of 4-QAM system outperformed that of the QPSK. As such, 4-QAM system achieves a greater distance more than all, this is because, in-between the adjacent points in the I-Q plane, the 4-QAM system distribute their points more evenly than the QPSK systems as can be seen from the Figure 15 and 21 during constellation and plotting.

3.Finally, low rate modulation schemes (QPSK and 4-QAM) shows a better Min-BER improvement than those of high rate modulation schemes (256-QAM and 512-QAM), though as the distance increases, the signal quality deteriorate more in high rate modulation.

5. CONCLUSION

The Percentage (%) Min. BER and Max. Q-factor improvements in CO-OFDM outperformed those of DDO-OFDM systems provided the same parameters were used throughout the simulation processes. This is a result of inherent advantages of CO-OFDM as against the DDO-OFDM systems. However, the next sets of simulation which involves the conventional (CO-OFDM) as against the proposed (CO-OFDM + PRM) system, the proposed system outperformed the conventional system provided the same parameters were used. The Phase Rotation Method (PRM) eliminates the residual dispersion left after chromatic dispersion and equalization.

6. ACKNOWLEDGEMENTS

The authors wish to express their sincere gratitude to the experts who developed the OptiSystem and MATLAB Softwares, which without them this work wouldn`t have been possible. Moreso, to the Head of the Department of Electrical/Electronics Engineering, Faculty of Engineering and Engineering Technology, Engr. Dr. I.T Thuku, Ph.D as well as the departmental Post Gradguate Coordinator, Engr. Dr. S.Y Musa, Ph.D, both from Modibbo Adama University of Technology, yola Adamawa State, Nigeria for their good counsel, encouragement, valuable suggestions, support and facilities rendered throughout this research work.

REFERENCES

[1] A. J. Lowery, L. Du, and J. Armstrong, "Orthogonal frequency division multiplexing for adaptive dispersion compensation in long haul WDM systems," in *Optical fiber communication conference*, 2006, p. PDP39.

[2] R. Giddings, X. Jin, E. Hugues-Salas, E. Giacoumidis, J. Wei, and J. Tang, "Experimental demonstration of a record high 11.25 Gb/s real-time optical OFDM transceiver supporting 25km SMF end-to-end transmission in simple IMDD systems," *Optics Express,* vol. 18, pp. 5541-5555, 2010.

[3] L. Nadal, J. M. Fàbrega, J. Vílchez, and M. S. Moreolo, "Experimental analysis of 8-QAM constellations for adaptive optical OFDM systems," *IEEE Photonics Technology Letters,* vol. 28, pp. 445-448, 2016.

[4] A. J. Lowery, L. B. Du, and J. Armstrong, "Performance of optical OFDM in ultralong-haul WDM lightwave systems," *Journal of Lightwave Technology,* vol. 25, pp. 131-138, 2007.

[5] M. Sandell, J. v. d. Beek, and P. O. Börjesson, "Timing and frequency synchronization in OFDM systems using the cyclic prefix," in *International Symposium on Synchronization: 14/12/1995-15/12/1995*, 1995, pp. 16-19.

[6] W. Shieh and C. Athaudage, "Coherent optical orthogonal frequency division multiplexing," *Electronics letters,* vol. 42, pp. 587-589, 2006.

[7] A. Yekani, S. Amiralizadeh, and L. A. Rusch, "Theoretical analysis of chromatic dispersion, phase noise, and SSBI in direct-detection single-side-band optical OFDM transmission," in *Photonics Conference (IPC), 2016 IEEE*, 2016, pp. 805-806.

[8] L. Zhang, S. Xiao, M. Bi, L. Liu, and Z. Zhou, "Channel estimation algorithm for interference suppression in IMDD–OQAM–OFDM transmission systems," *Optics Communications,* vol. 364, pp. 129-133, 2016.

[9] E. Giacoumidis, S. T. Le, I. Aldaya, J. Wei, M. McCarthy, N. Doran*, et al.*, "Experimental comparison of artificial neural network and volterra based nonlinear equalization for CO-OFDM," in *Optical Fiber Communications Conference and Exhibition (OFC), 2016*, 2016, pp. 1-3.

[10] J.-C. Kuo, C.-H. Wen, and A.-Y. Wu, "Implementation of a programmable 64/spl sim/2048-point FFT/IFFT processor for OFDM-based communication systems," in *Circuits and Systems, 2003. ISCAS'03. Proceedings of the 2003 International Symposium on*, 2003, pp. II-II.

[11] M. Zourob and R. Rao, "2× 1-D fast Fourier transform interpolation for LTE-A OFDM pilot-based channel estimation," in *Electrical and Computing Technologies and Applications (ICECTA), 2017 International Conference on*, 2017, pp. 1-5.

[12] S. T. Ahmad and K. P. Kumar, "Normalized LMS filter for chromatic dispersion compensation in single polarization 40Gbps CO-OFDM system in presence of timing and frequency offsets," *Optik-International Journal for Light and Electron Optics,* vol. 127, pp. 668-672, 2016.

[13] Y. Wang, J. Yu, and N. Chi, "Demonstration of 4$\times $128-Gb/s DFT-S OFDM Signal Transmission over 320-km SMF With IM/DD," *IEEE Photonics Journal,* vol. 8, pp. 1-9, 2016.

[14] S. Chen and C. Zhu, "ICI and ISI analysis and mitigation for OFDM systems with insufficient cyclic prefix in time-varying channels," *IEEE Transactions on Consumer Electronics,* vol. 50, pp. 78-83, 2004.

[15] E. Giacoumidis, S. Mhatli, T. Nguyen, S. T. Le, I. Aldaya, M. E. McCarthy*, et al.*,

"Comparison of DSP-based nonlinear equalizers for intra-channel nonlinearity compensation in coherent optical OFDM," *Optics letters,* vol. 41, pp. 2509-2512, 2016.

[16] W. Henkel, G. Taubock, P. Odling, P. O. Borjesson, and N. Petersson, "The cyclic prefix of OFDM/DMT-an analysis," in *Broadband Communications, 2002. Access, Transmission, Networking. 2002 International Zurich Seminar on*, 2002, pp. 22-22.

[17] F. Ramos, E. Vourc'h, and J. Marti, "Techniques for the Compensation for Chromatic-Dispersion Effects in Fiber-Wireless Systems," 1995.

[18] B. Lin, J. Li, H. Yang, Y. Wan, Y. He, and Z. Chen, "Comparison of DSB and SSB transmission for OFDM-PON," *IEEE/OSA Journal of Optical Communications and Networking,* vol. 4, pp. B94-B100, 2012.

[19] M. Sieben, J. Conradi, and D. E. Dodds, "Optical single sideband transmission at 10 Gb/s using only electrical dispersion compensation," *Journal of Lightwave Technology,* vol. 17, pp. 1742-1749, 1999.

[20] Ishiwu I. Jude, Yahya Adamu, Oguche D. Onoja, and B. Andrew, "Efficient Chromatic and Residual Dispersion Postcompensation for Coherent Optical OFDM," *International Journal of Science and Engineering Applications,* vol. 6, pp. 372-381, 2017.

[21] A. Gatto, S. Mandelli, J. Morosi, M. Magarini, P. Martelli, and P. Boffi, "Experimented phase noise limitations in directly-detected single side-band optical OFDM systems," in *Optical Fiber Communications Conference and Exhibition (OFC), 2017*, 2017, pp. 1-3.

[22] Ishiwu I. Jude, Yahaya Adamu , Mathew Luka, and A. Baams, "Optical-OFDM Detection Techniques," *International Journal of Science and Engineering Applications (IJSEA)* vol. Volume 7, pp. 23-33, 2018.